

## Supporting Information

# Evaluation of Excited-State Bond Weakening for Ammonia Synthesis from a Manganese Nitride: Stepwise Proton Coupled Electron Transfer is Preferred over Hydrogen Atom Transfer

Florian Loose,<sup>a</sup> Dian Wang,<sup>a</sup> Lei Tian,<sup>a</sup> Gregory D. Scholes,<sup>a</sup> Robert R. Knowles<sup>a</sup> and Paul J. Chirik<sup>a,\*</sup>

Department of Chemistry, Princeton University  
Frick Laboratory, Princeton, 08544 (USA)  
E-mail: pchirik@princeton.edu

### Table of Contents

Experimental Procedures	S2
I. General Considerations	S2
II. Preparation of the Ruthenium Complexes <b>1a,b</b>	S3
III. Preparation of the Manganese Complex <b>3</b>	S4
IV. General Catalytic Procedure	S5
V. <sup>15</sup> N Labeling Experiment	S8
VI. Stern-Volmer Quenching Studies	S9
VII. Spectroscopic Data	S10
References	S20

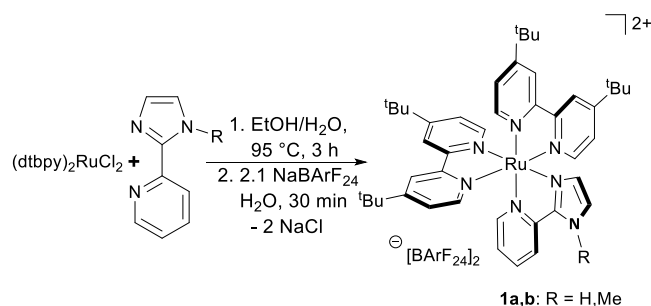
## Experimental Procedures

### I. General Considerations

All air- and moisture-sensitive manipulations were carried out using vacuum line, Schlenk and cannula techniques or in an MBraun inert atmosphere (nitrogen) dry box unless otherwise noted. All glassware was stored in a pre-heated oven prior to use. The solvents used for air- and moisture-sensitive manipulations were dried and deoxygenated using literature procedures.<sup>[1]</sup> (dtbpy)<sub>2</sub>RuCl<sub>2</sub>,<sup>[2]</sup> (tBuSalen)MnN,<sup>[3]</sup> 2-(1-methyl-1H-imidazol-2-yl)pyridine<sup>[4]</sup> and NaBArF<sub>24</sub><sup>[5]</sup> were prepared according to literature procedures NMR spectra were recorded on either a Bruker ADVANCE 300, 500 or Varian Inova I400 spectrometer. All <sup>1</sup>H and <sup>13</sup>C NMR chemical shifts are reported in ppm relative to SiMe<sub>4</sub> using the residual solvent signal as internal reference.<sup>[6]</sup> <sup>19</sup>F NMR spectra were referenced to CFC<sub>3</sub> as an external standard. Continuous wave EPR spectra were recorded at room temperature on an X-band Bruker EMXPlus spectrometer equipped with an EMX standard resonator and a Bruker PremiumX microwave bridge. Luminescence quenching experiments were conducted on an Agilent Cary Eclipse Fluorescence Spectrometer. Cyclic voltammograms (CV) were collected in THF solution (1 mM in compound) with [<sup>t</sup>Bu<sub>4</sub>N][PF<sub>6</sub>] (0.2 M), using a 3 mm glassy carbon working electrode, platinum wire as the counter electrode, and silver wire as the reference in a drybox equipped with electrochemical outlets. CVs were recorded using a BASi EC Epsilon electrochemical workstation and analyzed using the BASi Epsilon-EC S4 software. All CVs were run at 23 °C. Potentials are reported versus Cp<sub>2</sub>Fe/Cp<sub>2</sub>Fe<sup>+</sup> and were obtained using the *in-situ* method. Elemental analyses were performed at Robinson Microlit Laboratories, Inc., in Ledgewood, NJ.

Absorption spectra were recorded on a Cary 60 UV-Vis spectrometer (Agilent Technologies) with an integration time of 0.1 s and a data interval of 1 nm. Absorption measurements were done using a 2 mm cuvette fitted with a J-Young valve and sealed with a Teflon cap, for which the maximum absorbance in the visible region of the solution was never above 0.5 OD. Emission and excitation spectra were recorded on a QuantaMaster 400 (HORIBA Scientific, NJ), with excitation and emission slit widths of 1 nm and an integration time of 1 s. Emission measurements were done using a 10 mm J-Young cuvette, for which the maximum absorbance in the visible region of the solution was never above 0.1 OD to avoid any inner filter effects. Excited-state lifetime was determined using time-correlated single photon counting (TCSPC) and nanosecond transient absorption spectroscopy. TCSPC measurements were done on a DeltaFlex TCSPC system (Horiba Scientific, NJ) photoexcited with DeltaDiode using a 10 mm J-Young cuvette, for which the absorbance at the excitation wavelength of the solution was below 0.05 OD to ensure single photon emission behavior. The pulse duration of the excitation laser diodes (406 & 507 nm) were less than 200 ps, which is significantly shorter than the excited-state lifetime of the measured species therefore justifies the use of single-exponential fitting method for post-processing the time-resolved data. Nanosecond transient absorption measurements were done on a transient absorption spectrometer with commercial modules assembled in house. A detailed primer for transient absorption spectroscopy can be found elsewhere.<sup>[7]</sup> For the purpose of excited-state lifetime measurement, the output pulse of a 1kHz regeneratively amplified Ti:Sapphire laser (Coherent Libra, Santa Clara, California), centered at 800 nm with a pulse duration of approximately 45 fs and output power of 3.6 W, is reflected with 90-10 beamsplitter into a commercial optical parametric amplifier (OPerA Solo, Vilnius, Lithuania) to generate a narrowband pump light at 500 nm, which is chopped at 500 Hz and then focused into the sample position inside a commercial transient absorption spectrometer (Ultrafast Systems Helios, Sarasota, Florida). The supercontinuum probe pulse is generated using a commercial photonic crystal fiber (Ultrafast Systems EOS, Sarasota, Florida) which is synchronized with the Ti:Sapphire laser and electronically delayed to realize a time window from 500 picoseconds to 400 milliseconds. The samples were prepared in a 2 mm J-Young cuvette for which the absorbance at pump wavelength was below 0.4 OD. Pre and post scan absorption measurements were performed to make sure the photodegradation was minimal during the measurement. No severe degradation was found for all measured samples. The resultant data were background subtracted by subtracting the averaged transient absorption spectra before time zero. The excited-state lifetime was then determined by single-exponentially fitting the single wavelength trace at the excited-state absorption (ESA) and ground-state bleaching (GSB) regions of the transient spectra.

## II. Preparation of the Ruthenium Complexes 1a,b.



**Scheme S1.** Synthesis of the ruthenium complexes **1a,b** (dtbpy = 4,4'-Di-*tert*-butyl-2,2'-bipyridine).

**Preparation of 1a,b.** **1a,b** were prepared analog to a literature procedure.<sup>[8]</sup> A solution of (dtbpy)<sub>2</sub>RuCl<sub>2</sub> (1.0 eq) and the corresponding pyridine imidazole (1.1 eq) in a 1:1 mixture of ethanol and water (24 ml/mmol) was degassed three times and refluxed for 3 h under a nitrogen atmosphere. After cooling the reaction mixture to room temperature a few drops of concentrated aqueous HCl were added and the ethanol was removed under reduced pressure. 2.1 eq NaBArF suspended in water (20 ml/mmol) were added resulting in the precipitation of an orange solid. This suspension was stirred for 30 min at room temperature, the precipitate filtered off and washed three times with water. Recrystallisation from a mixture of methanol and water yields **1a** respectively **1b** as orange solids.

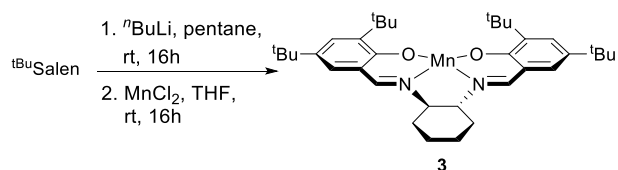
Analytical data for **1a**:

Yield: 311 mg (0.12 mmol, 50 %). Anal Calcd for C<sub>108</sub>H<sub>79</sub>B<sub>2</sub>F<sub>48</sub>N<sub>7</sub>Ru: C, 51.69; H, 3.17; N, 3.91. Found: C, 51.49; H, 3.06; N, 3.71. <sup>1</sup>H NMR (399.8 MHz, 298 K, THF-*d*8): δ 1.36 (s, 9H), 1.37 (s, 9H), 1.38 (m, 18H), 6.56 (s, 1H), 7.28-7.38 (m, 2H), 7.43-7.51 (m, 4H), 7.54 (s, 8H), 7.62-7.65 (m, 2H), 7.71 (d, 1H, <sup>3</sup>J<sub>H,H</sub> = 6.0 Hz), 7.76-7.77 (m, 16H), 7.80-7.82 (m, 1H), 7.96-8.05 (m, 3H), 8.56-8.59 (m, 4H), 13.48 (s, 1H). <sup>19</sup>F{<sup>1</sup>H} NMR (376.2 MHz, 300 K, THF-*d*8): δ -63.4.

Analytical data for **1b**:

Yield: 475 mg (0.19 mmol, 75 %). Anal Calcd for C<sub>109</sub>H<sub>81</sub>B<sub>2</sub>F<sub>48</sub>N<sub>7</sub>Ru: C, 51.88; H, 3.24; N, 3.89. Found: C, 51.85; H, 3.08; N, 4.05. <sup>1</sup>H NMR (399.8 MHz, 300 K, THF-*d*8): δ 1.35 (s, 9H), 1.36 (s, 9H), 1.38 (m, 18H), 4.23 (s, 3H), 6.45 (d, 1H, <sup>3</sup>J<sub>H,H</sub> = 1.4 Hz), 7.30-7.33 (m, 1H), 7.43 (dd, 1H, <sup>3</sup>J<sub>H,H</sub> = 2.1 Hz, <sup>3</sup>J<sub>H,H</sub> = 6.1 Hz), 7.47-7.50 (m, 3H), 7.54 (s, 8H), 7.62 (d, 1H, <sup>3</sup>J<sub>H,H</sub> = 6.0 Hz), 7.68-7.73 (m, 5H), 7.76-7.77 (m, 16H), 8.02 (dt, 1H, <sup>3</sup>J<sub>H,H</sub> = 1.4 Hz, <sup>3</sup>J<sub>H,H</sub> = 8.0 Hz), 8.33 (d, 1H, <sup>3</sup>J<sub>H,H</sub> = 8.3 Hz), 8.55-8.59 (m, 4H). <sup>19</sup>F{<sup>1</sup>H} NMR (376.2 MHz, 300 K, THF-*d*8): δ -63.4.

### III. Preparation of the Manganese Complex **3**.



#### Scheme S2. Synthesis of (<sup>t</sup>BuSalen)Mn **3**.

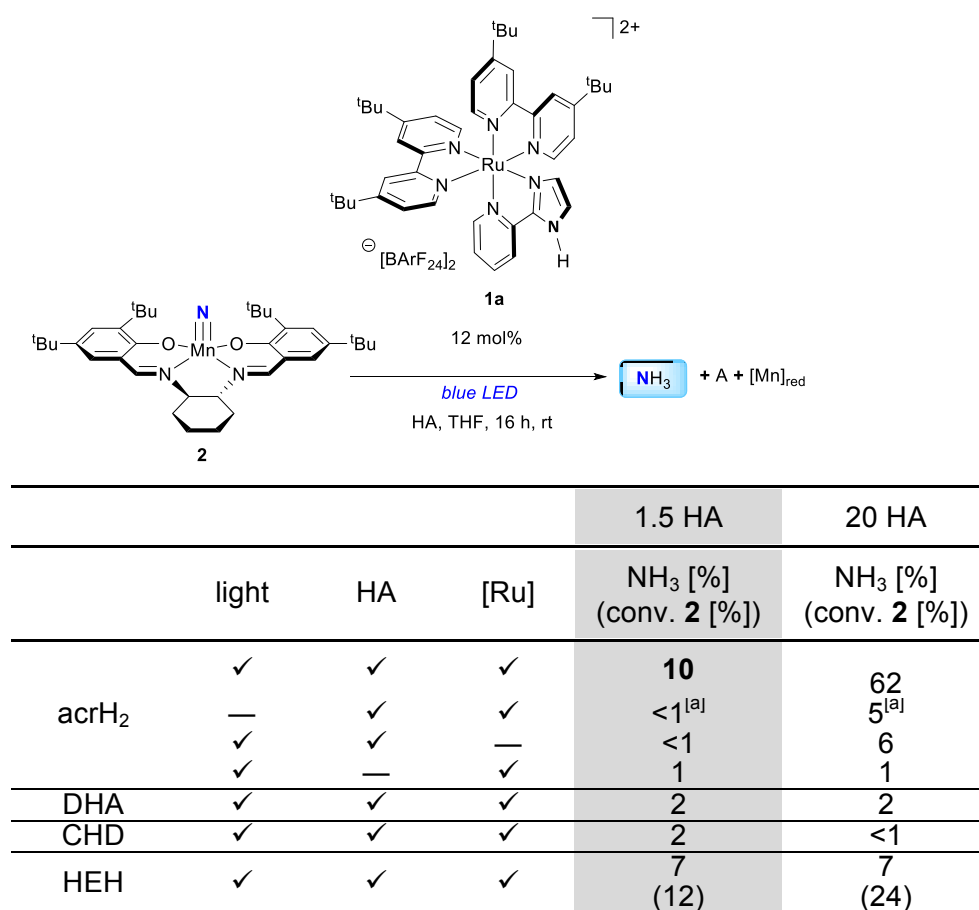
**Preparation of **3**.** To a solution of 273 mg (0.5 mmol) <sup>t</sup>BuSalen in 5 ml pentane 625  $\mu$ l (1.0 mmol) <sup>n</sup>BuLi (1.6 M, hexanes) were added dropwise at room temperature. The reaction mixture was stirred 16 h at room temperature, filtered and the solids were washed three times with 10 ml pentane. Drying the slightly yellow solids in vacuum yields 259 mg (0.46 mmol, 92 %) of the lithium salt Li<sub>2</sub><sup>t</sup>BuSalen which was directly used for the subsequent synthesis of **3**. To 13 mg (0.1 mmol) MnCl<sub>2</sub> and 56 mg (0.1 mmol) of Li<sub>2</sub><sup>t</sup>BuSalen were added 5 ml THF and the reaction mixture was stirred 16 h at room temperature. After evaporating the solvent, the residue was suspended in 3 ml toluene, filtered over celite and the solids were washed three times with 1 ml toluene. Removal of the solvent in vacuum yields 60 mg (0.1 mmol, quantitative) of **3** as yellow-orange solid. Anal Calcd for C<sub>36</sub>H<sub>52</sub>MnN<sub>2</sub>O<sub>2</sub>: C, 72.09; H, 8.74; N, 4.67. Found: C, 71.93; H, 8.64; N, 4.45.

**Conversion of **3** to **2**.** A solution of 60 mg (0.10 mmol) **3** and 50 mg (0.21 mmol) C<sub>2</sub>Cl<sub>6</sub> in 5 ml THF was stirred 16 h at room temperature. After removal of all volatiles the residue was washed three times with 2 ml pentane and dried in vacuum yielding a brown solid. This solid was dissolved in a mixture of 4 ml dichloromethane and 1 ml methanol. 0.1 ml NH<sub>4</sub>OH (14.5 M, H<sub>2</sub>O) were added, the reaction mixture stirred 15 min at room temperature and 0.3 ml NaOCl (10 %, H<sub>2</sub>O) were added dropwise. After stirring the reaction mixture 8 h at room temperature the organic layer was separated, washed four times with 3 ml H<sub>2</sub>O, dried over MgSO<sub>4</sub> and evaporated to dryness yielding 38 mg (0.06 mmol, 60 %) of a green solid that was identified by <sup>1</sup>H-NMR spectroscopy as **2**.

## IV. General Catalytic Procedure

**General procedure for the photocatalytic formation of ammonia from 2.** In a typical experiment 6 mg (10  $\mu\text{mol}$ ) of **2**, the corresponding amount of the stoichiometric proton and electron source (table S1 – S3) and 3 mg (1.2  $\mu\text{mol}$ ) of the photocatalyst were dissolved in 5 ml of solvent (table S1 – S3). Afterwards the reaction mixture was stirred 16 h under irradiation with two Kessil™ H-150 blue lamps (30 W) using a household fan to keep the reaction mixture at a constant temperature. In control experiments in the dark, the reaction vessel was wrapped in aluminum foil and the reaction mixture was stirred at 45 °C for 24 h, instead. After the reaction, all volatiles were transferred to 1 ml HCl (2 M, Et<sub>2</sub>O). After the removal of the solvent of the Et<sub>2</sub>O solution, the residue was analyzed by the indophenol method<sup>[9]</sup> to quantify the amount of ammonia formed.

**Table S1.** Optimization of the stoichiometric proton and electron source for the photocatalytic formation of ammonia from the manganese nitride **2**.



[a] 45 °C, 24 h.

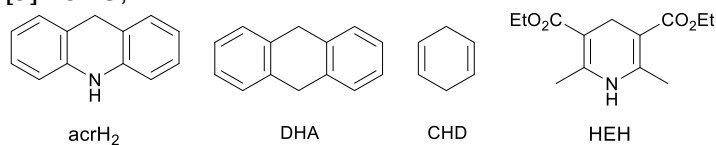
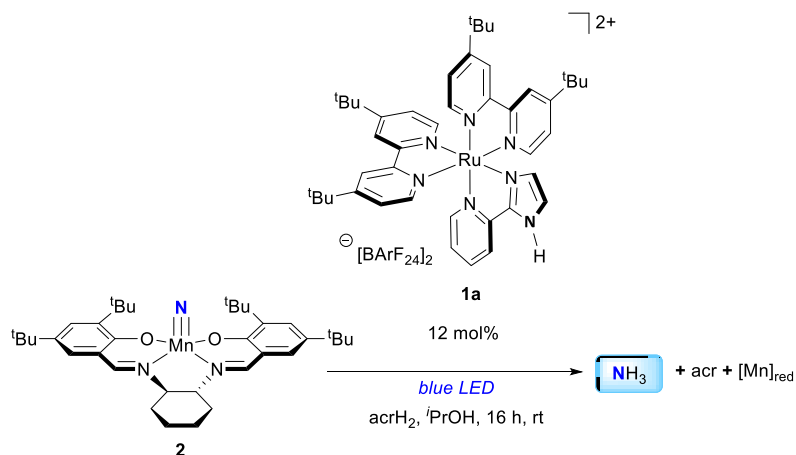


**Table S2.** Optimization of the amount of stoichiometric proton and electron source for the photocatalytic formation of ammonia from the manganese nitride **2**.



light	$\text{acrH}_2$	[Ru]	1.5 $\text{acrH}_2$	10 $\text{acrH}_2$	20 $\text{acrH}_2$
			$\text{NH}_3$ [%]	$\text{NH}_3$ [%]	$\text{NH}_3$ [%]
✓	✓	✓	<b>27</b>	<b>62</b>	<b>80</b>
—	✓	✓	<1 <sup>[a]</sup>	3 <sup>[a]</sup>	3 <sup>[a]</sup>
✓	✓	—	4	13	21
—	✓	—			2
✓	—	✓	3	3	3

[a] 45 °C, 24 h.

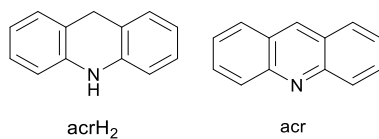
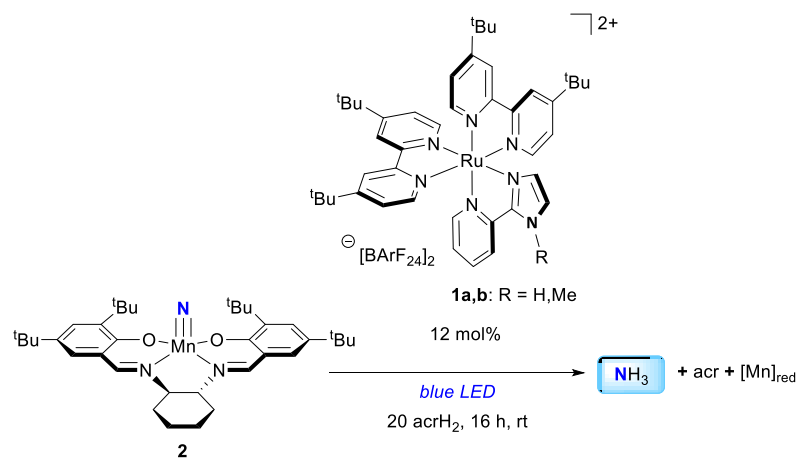
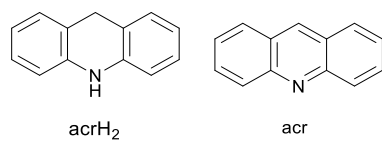


**Table S3.** Catalytic formation of ammonia from the manganese nitride **2**.



light	$\text{acrH}_2$	[Ru]	$\text{NH}_3$ [%]			
			R = H		R = Me	
			<i>i</i> PrOH	THF	<i>i</i> PrOH	THF
✓	✓	✓	80	62	72	80
—	✓	✓	3 <sup>[a]</sup>	5 <sup>[a]</sup>	2 <sup>[a]</sup>	<1 <sup>[a]</sup>
✓	—	✓	3	1	9	<1
✓	✓	—	21	6	21	6
—	✓	—	2	<1	2	<1

[a] 45 °C, 24 h.



## V. $^{15}\text{N}$ Labeling Experiment

**Procedure for the photocatalytic formation of ammonia from  $^{15}\text{N}$  labeled **2**.** 6 mg (10  $\mu\text{mol}$ ) of  $^{15}\text{N}$  labeled **2**, 36 mg (0.2 mmol)  $\text{acrH}_2$  and 3 mg (1.2  $\mu\text{mol}$ ) **1a** were dissolved in 5 ml of  $\text{PrOH}$ . Afterwards the reaction mixture was stirred 16 h under irradiation with two Kessil<sup>TM</sup> H-150 blue lamps (30 W) using a household fan to keep the reaction mixture at a constant temperature. After the reaction, all volatiles were transferred to 1 ml  $\text{HCl}$  (2 M,  $\text{Et}_2\text{O}$ ). After the removal of the solvent of the  $\text{Et}_2\text{O}$  solution, the residue was analyzed by  $^1\text{H}$ -NMR spectroscopy in  $\text{DMSO-}d_6$  with 5  $\mu\text{l}$  (63.46  $\mu\text{mol}$ )  $\text{C}_2\text{H}_4\text{Cl}_2$  as internal standard. Yield ( $^{15}\text{NH}_3$ ): 8.21  $\mu\text{mol}$  (82 %).

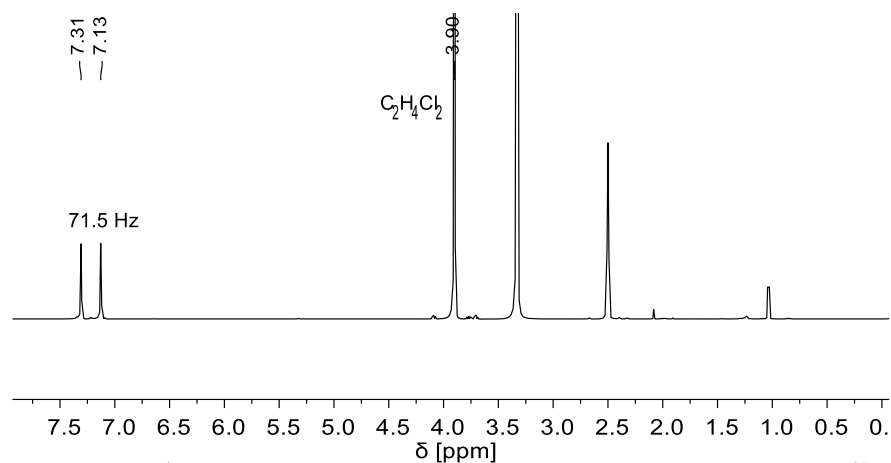


**Figure S1.**  $^1\text{H}$ -NMR spectrum (399.8 MHz, 298 K,  $\text{DMSO-}d_6$ ) of  $^{15}\text{NH}_4\text{Cl}$  from the photocatalytic reaction of  $^{15}\text{N}$  labeled **2**.

## VI. Stern-Volmer Quenching Studies

Stern-Volmer luminescence quenching studies were carried out using a  $8 \times 10^{-5}$  M solution of **1a** in iPrOH or a  $1 \times 10^{-4}$  M solution of **1b** in THF and variable concentrations of 9,10-dihydroacridine (acrH<sub>2</sub>) respectively **2** at room temperature under a nitrogen atmosphere. The samples were prepared in quartz cuvettes inside a N<sub>2</sub>-filled glovebox. The solutions were irradiated at 453 nm (**1a**) or 450 nm (**1b**) and the luminescence was measured at 640 nm (**1a**) or 630 nm (**1b**). The ratio of  $I_0/I$  was plotted as a function of the concentration of acrH<sub>2</sub> respectively **2**.

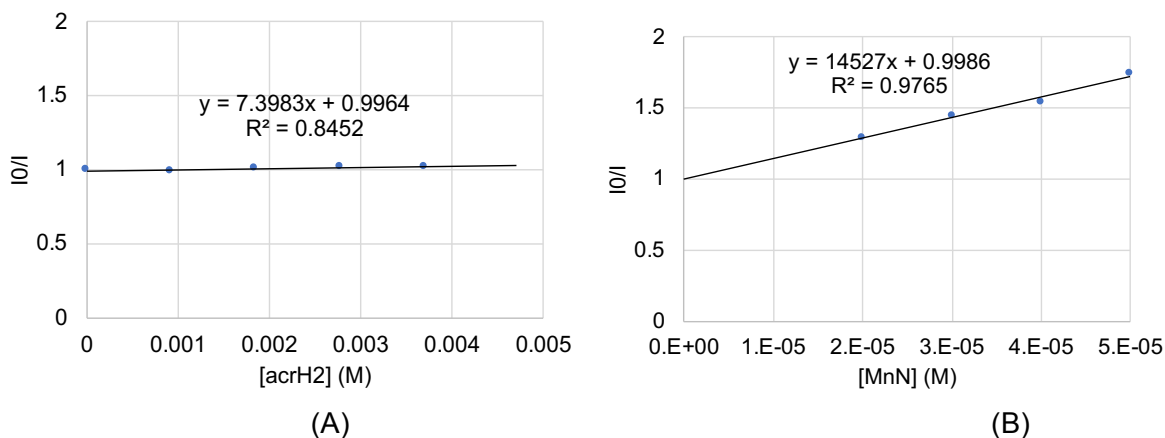


**Figure S2.** (A) Stern-Volmer plot of **1a** varying the concentration of acrH<sub>2</sub>. Conditions:  $8 \times 10^{-5}$  M **1a**, iPrOH,  $\lambda_{\text{exc}} = 453$  nm,  $\lambda_{\text{em}} = 640$  nm. (B) Stern-Volmer plot of **1a** varying the concentration of **2**. Conditions:  $8 \times 10^{-5}$  M **1a**, iPrOH,  $\lambda_{\text{exc}} = 453$  nm,  $\lambda_{\text{em}} = 640$  nm.

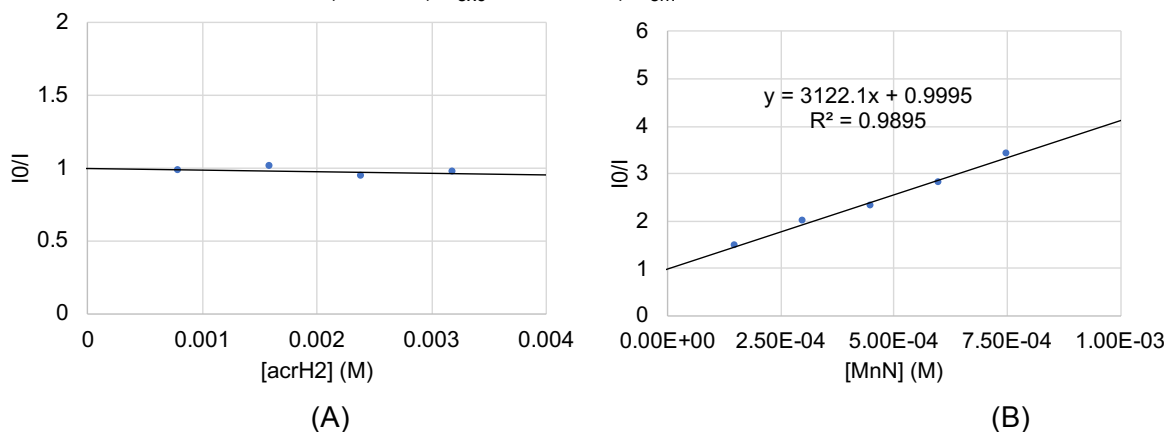


**Figure S3.** (A) Stern-Volmer plot of **1b** varying the concentration of acrH<sub>2</sub>. Conditions:  $1 \times 10^{-4}$  M **1b**, THF,  $\lambda_{\text{exc}} = 450$  nm,  $\lambda_{\text{em}} = 630$  nm. (B) Stern-Volmer plot of **1b** varying the concentration of **2**. Conditions:  $1 \times 10^{-4}$  M **1b**, THF,  $\lambda_{\text{exc}} = 450$  nm,  $\lambda_{\text{em}} = 630$  nm.

## VII. Spectroscopic Data

### Spectroscopic data of 1a.

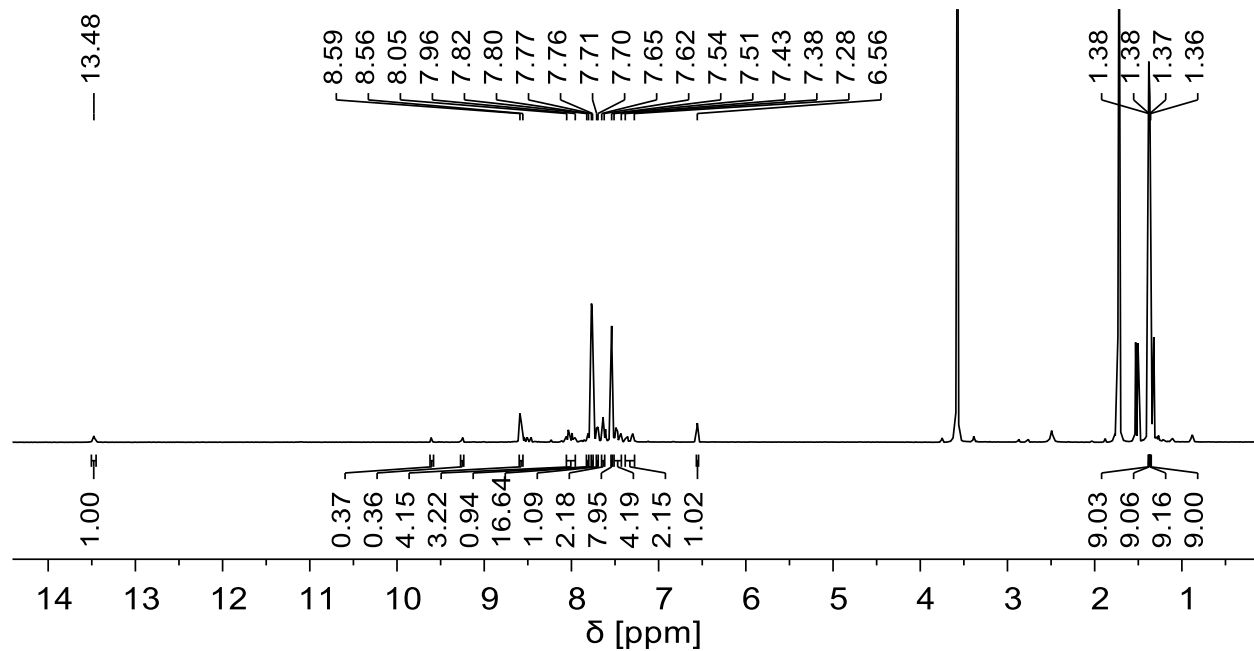


Figure S4.  $^1\text{H-NMR}$  spectrum (399.8 MHz, 298 K, THF- $d_8$ ) of 1a.

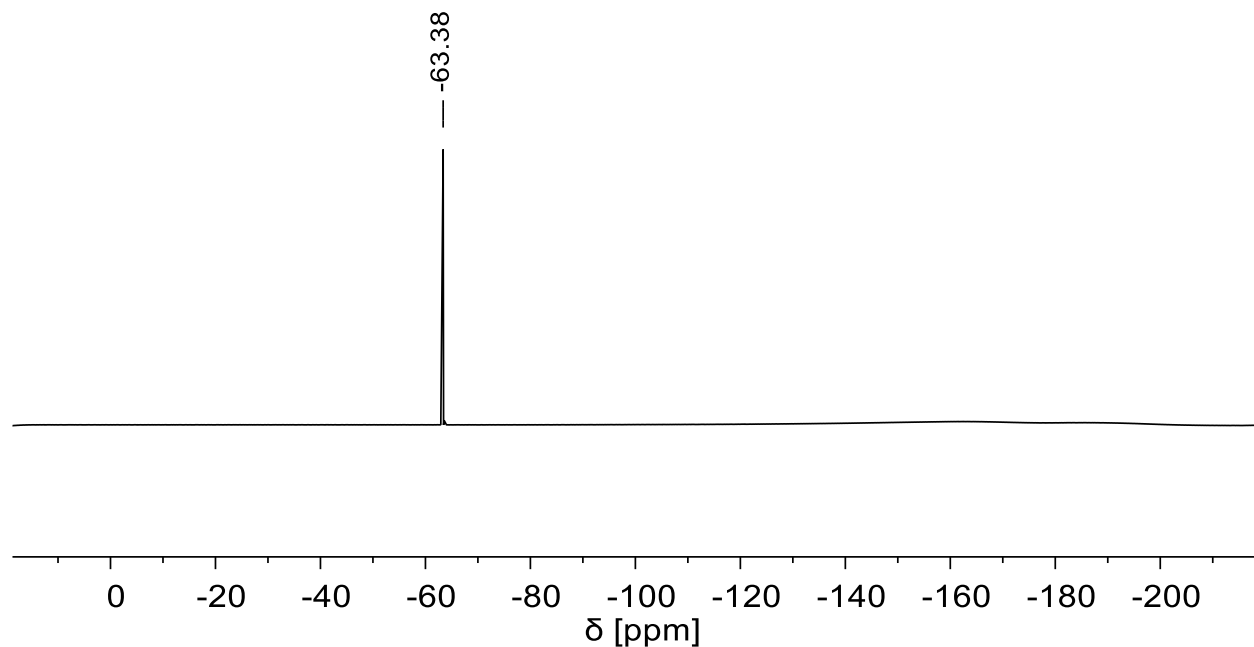
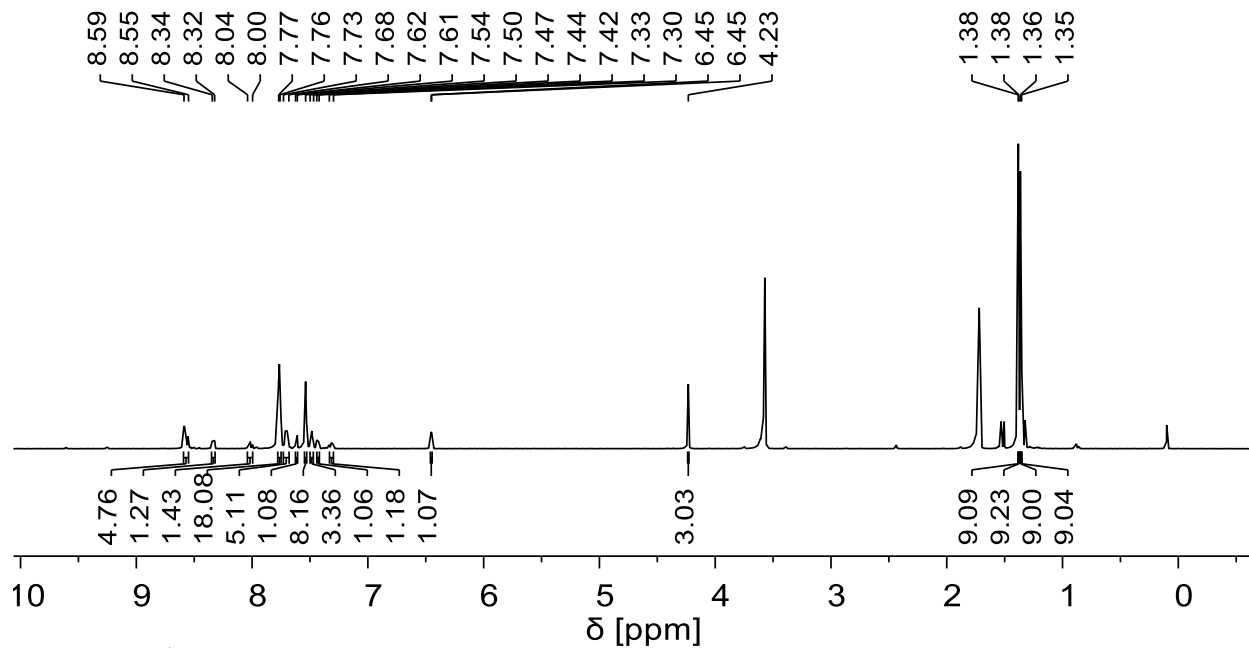
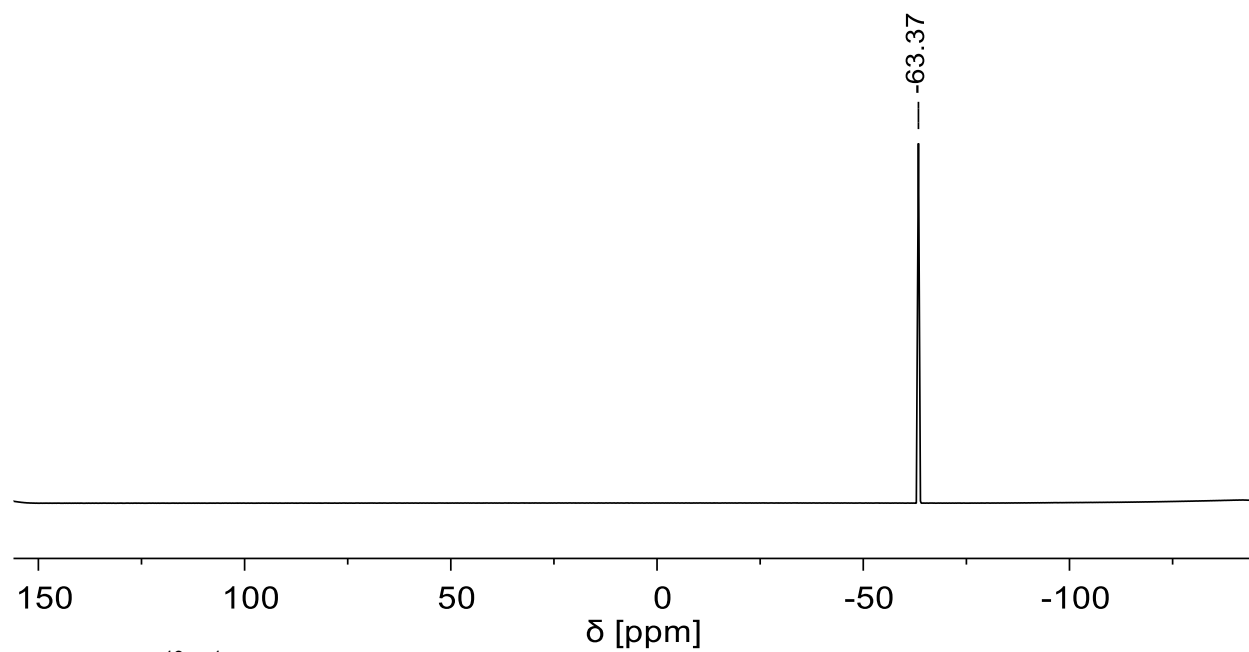


Figure S5.  $^{19}\text{F}\{^1\text{H}\}$ -NMR spectrum (376.2 MHz, 300 K, THF- $d_8$ ) of 1a.

**Spectroscopic data of 1b.**



**Figure S6.** <sup>1</sup>H-NMR spectrum (399.8 MHz, 300 K, THF-*d*8) of **1b**.



**Figure S7.** <sup>19</sup>F{<sup>1</sup>H}-NMR spectrum (376.2 MHz, 300 K, THF-*d*8) of **1b**.

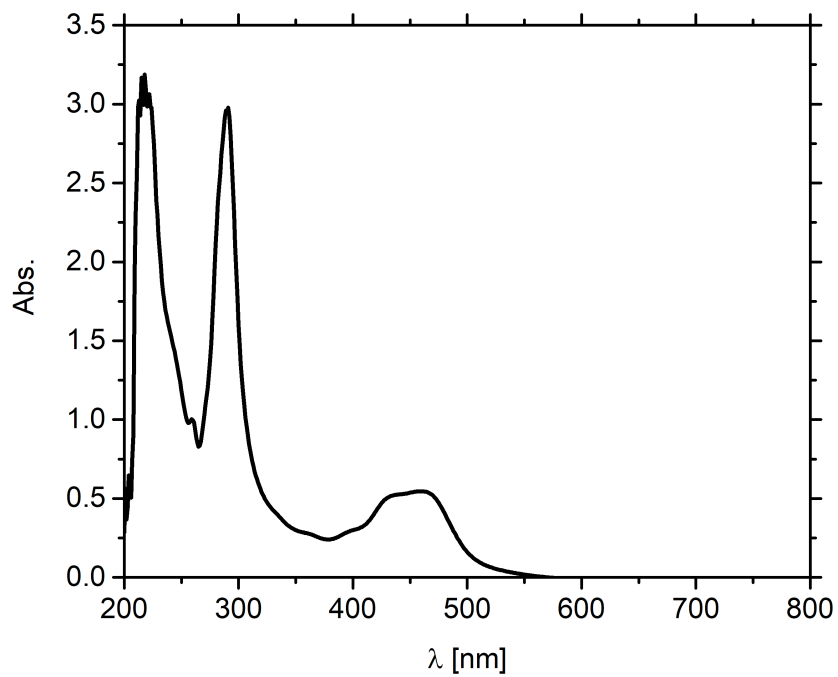


**Figure S8.** UV-VIS absorption spectrum of **1b** (40  $\mu$ M, 298 K, THF).

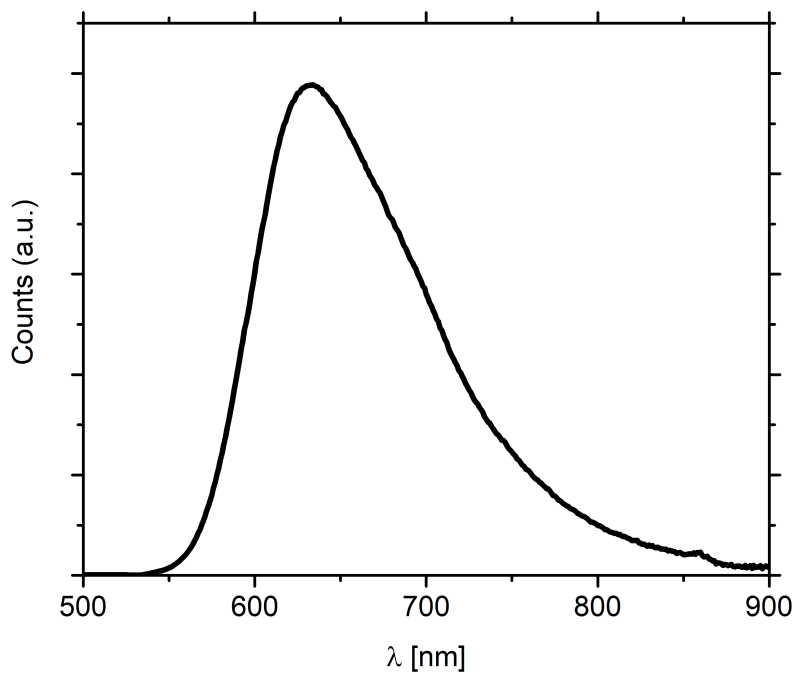


**Figure S9.** Emission spectrum of **1b** (10  $\mu$ M, 298 K, THF,  $\lambda_{\text{exc}} = 460$  nm).

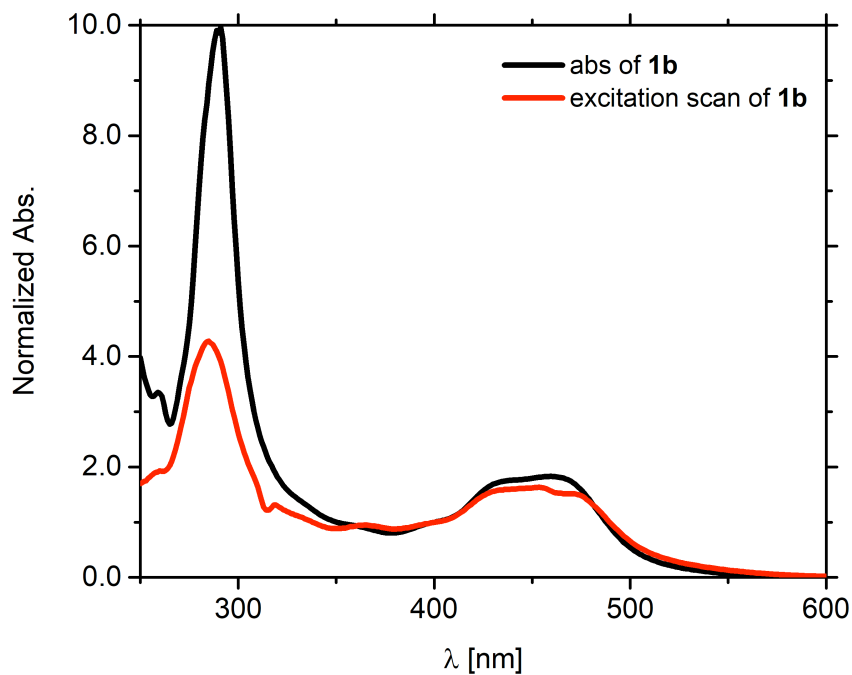


**Figure S10.** Excitation spectrum of **1b** (10  $\mu$ M, 298 K, THF,  $\lambda_{em}$  = 630 nm). Note that the excitation spectrum perfectly matches the absorption spectrum of **1b** in the visible region.

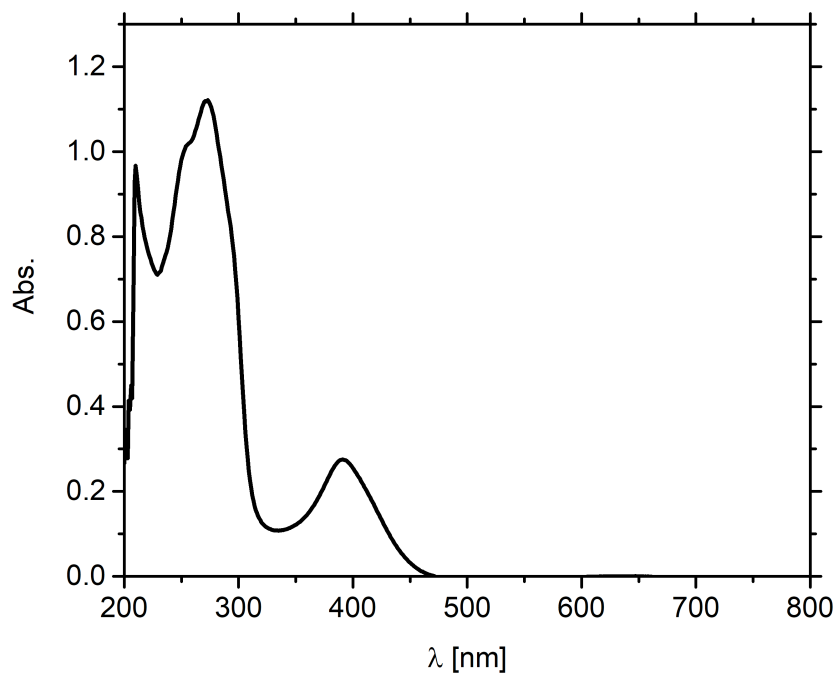


**Figure S11.** UV-VIS absorption spectrum of **2** (40  $\mu$ M, 298 K, THF).

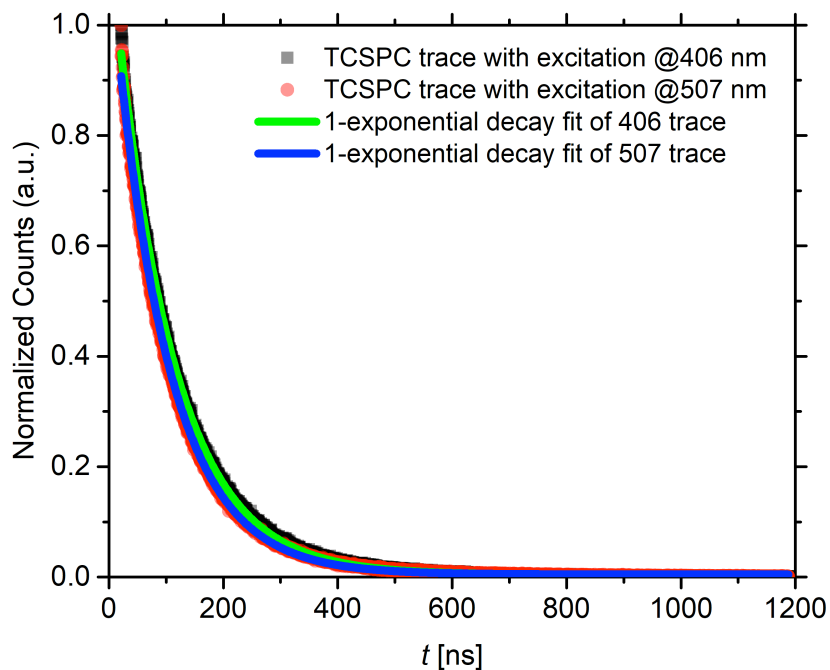


**Figure S12.** Time-correlated single photon counting data of **1b** (10  $\mu\text{M}$ , 298 K, THF,  $\lambda_{\text{exc}} = 406/507$  nm,  $\lambda_{\text{em}} = 630$  nm). All decay curves are first normalized at time zero and then fitted with 1-exponential decay:  $y = y_0 + A_1 e^{-t/\tau_1}$ . Fit results are: a) for 406 nm trace,  $A_1 = 1.1658 \pm 0.0008$ ,  $\tau_1 = 102.2 \pm 0.1$  (ns),  $y_0 = 0.0039 \pm 0.0001$ ; b) for 507 nm trace,  $A_1 = 1.131 \pm 0.001$ ,  $\tau_1 = 95.6 \pm 0.1$  (ns),  $y_0 = 0.0045 \pm 0.0001$ .

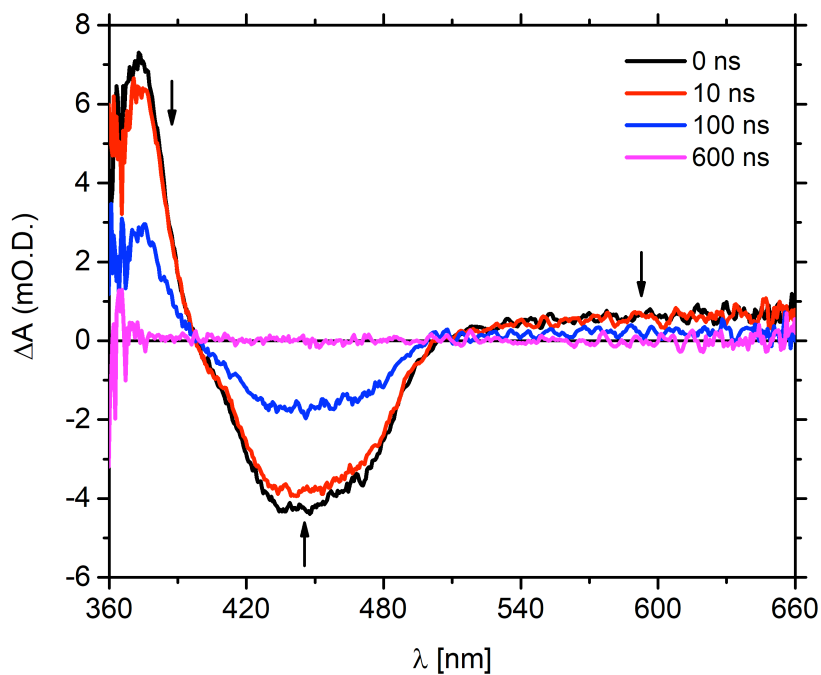


**Figure S13.** Nanosecond transient absorption spectra of **1b** (300  $\mu\text{M}$ , 298 K, THF,  $\lambda_{\text{pump}} = 500$  nm,  $P_{\text{pump}} = 300 \mu\text{W}$ ). Excited-state absorption and ground-state bleaching signals all die out with the same rate, suggesting that on this timescale, only one dynamic process is happening which is the decay to the ground-state from the  $^3\text{MLCT}$  state of **1b**.

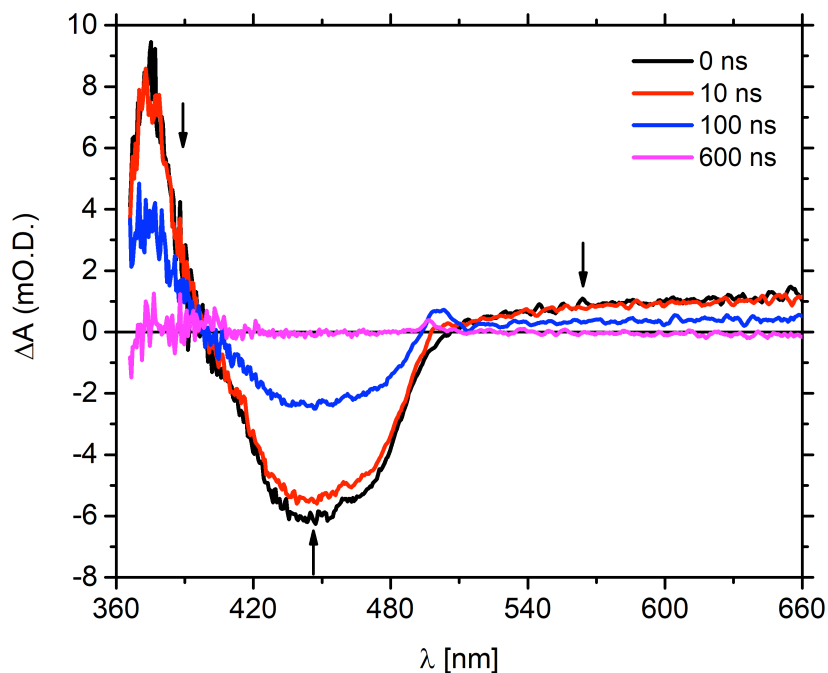


**Figure S14.** Nanosecond transient absorption spectra of **1b & 2** mixture ( $[\mathbf{1b}] = 300 \mu\text{M}$ ,  $[\mathbf{2}] = 815 \mu\text{M}$ , 298 K, THF,  $\lambda_{\text{pump}} = 500$  nm,  $P_{\text{pump}} = 400 \mu\text{W}$ ). The small peaks at 500 nm are due to pump scattering. The excited-state dynamics of **1b** doesn't change even when **2** is present in the solution, suggesting a static quenching mechanism between **1b** and **2**.

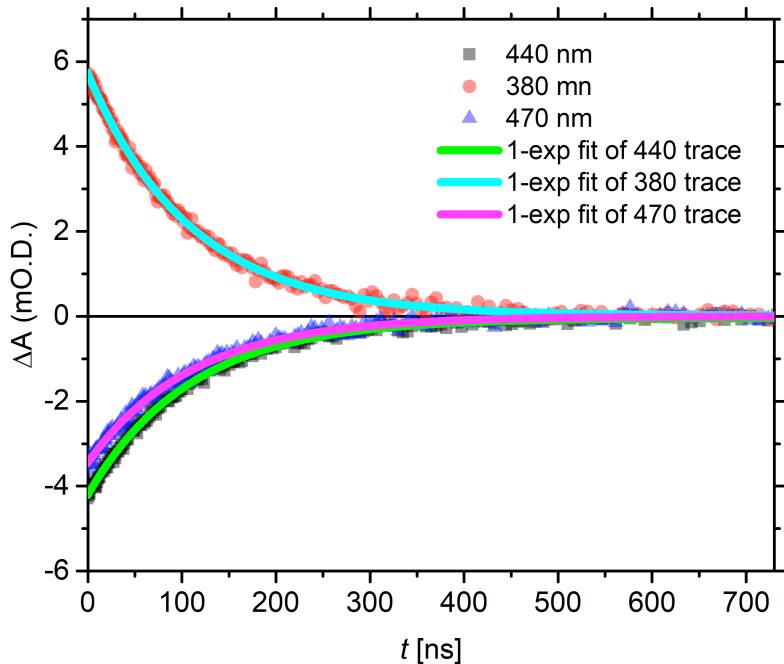


**Figure S15.** Single wavelength traces of nanosecond transient absorption spectra of **1b** (300  $\mu$ M, 298 K, THF, pump). All decay curves are fitted with 1-exponential decay:  $\Delta A = A_1 \exp(-t/t_1) + y_0$ . Fit results are: a) for 440 nm trace,  $A_1 = -0.00416 \pm 0.00002$ ,  $t_1 = 109 \pm 1$  (ns),  $y_0 = -0.00004 \pm 0.00001$ ; b) for 380 nm trace,  $A_1 = 0.00570 \pm 0.00002$ ,  $t_1 = 109 \pm 1$  (ns),  $y_0 = 0.00001 \pm 0.00001$ ; c) for 470 nm trace,  $A_1 = -0.00344 \pm 0.00002$ ,  $t_1 = 110 \pm 1$  (ns),  $y_0 = 0.00001 \pm 0.00001$ .

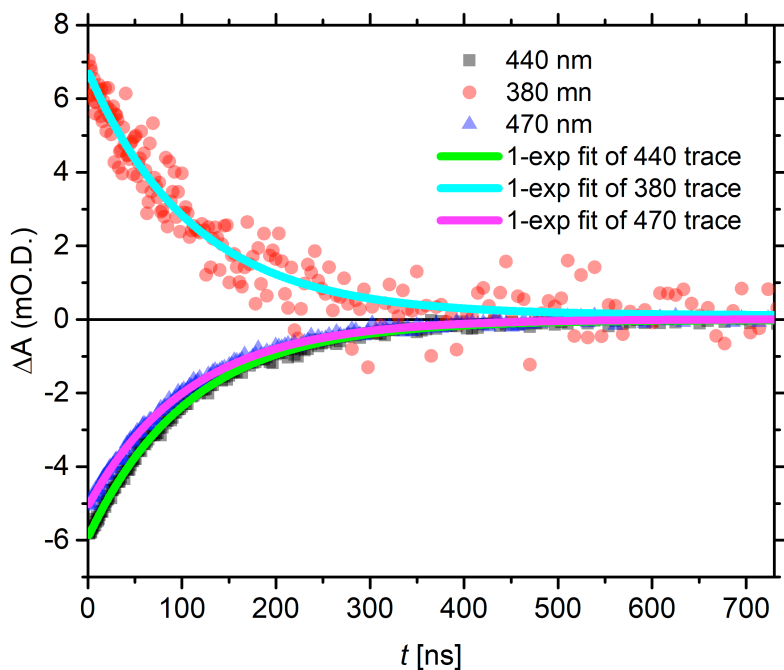


**Figure S16.** Single wavelength traces of nanosecond transient absorption spectra of **1b & 2** mixture ( $[1b] = 300 \mu\text{M}$ ,  $[2] = 815 \mu\text{M}$ , 298 K, THF, pump). All decay curves are fitted with 1-exponential decay:  $y = y_0 + A_1 \exp(-t/\tau_1)$ . Fit results are: a) for 440 nm trace,  $A_1 = -0.00591 \pm 0.00002$ ,  $\tau_1 = 109 \pm 1$  (ns),  $y_0 = -0.00002 \pm 0.00001$ ; b) for 380 nm trace,  $A_1 = 0.00570 \pm 0.00002$ ,  $\tau_1 = 112 \pm 6$  (ns),  $y_0 = 0.0001 \pm 0.0001$ ; c) for 470 nm trace,  $A_1 = -0.00508 \pm 0.00002$ ,  $\tau_1 = 108 \pm 1$  (ns),  $y_0 = 0.00001 \pm 0.00001$ .

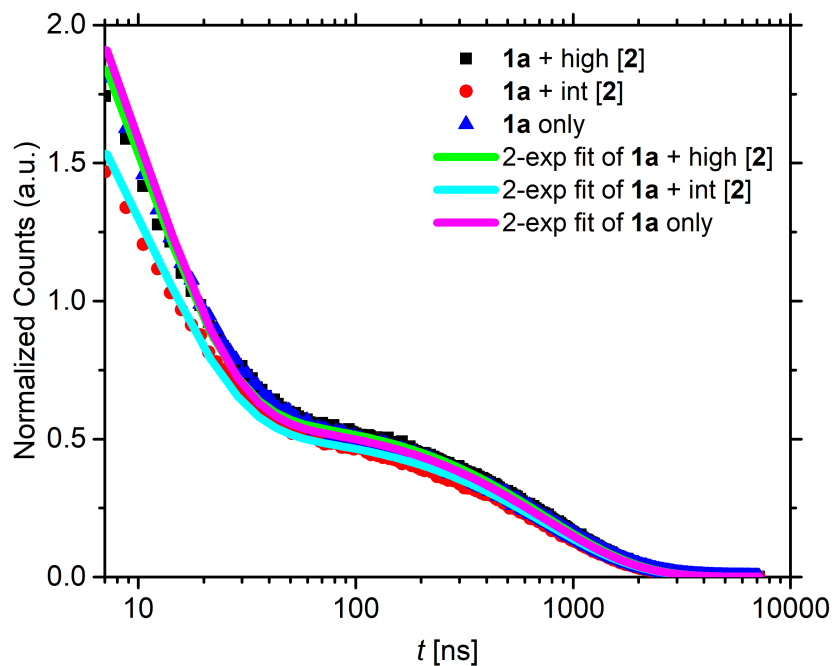


**Figure S17.** Dynamic Stern-Volmer experiment of **1a** & **2** measured with time-correlated single photon counting (**1a** 10  $\mu\text{M}$ , concentration of **2**: high [**2**] case 108  $\mu\text{M}$ , int [**2**] case 55  $\mu\text{M}$ , 298 K, THF,  $\lambda_{\text{exc}} = 406 \text{ nm}$ ,  $\lambda_{\text{em}} = 625 \text{ nm}$ ). All decay curves are fitted with 2-exponential decay:  $y = A_1 * \exp(-x/t_1) + A_2 * \exp(-x/t_2) + y_0$ . Fit results are: a) for **1a** + high [**2**],  $A_1 = 25114 \pm 48$ ,  $t_1 = 10.34 \pm 0.03 \text{ (ns)}$ ,  $A_2 = 5867 \pm 8$ ,  $t_2 = 754 \pm 1 \text{ (ns)}$ ,  $y_0 = 10 \pm 1$ ; b) for **1a** + int [**2**],  $A_1 = 19309 \pm 37$ ,  $t_1 = 11.00 \pm 0.03 \text{ (ns)}$ ,  $A_2 = 5302 \pm 6$ ,  $t_2 = 741 \pm 1 \text{ (ns)}$ ,  $y_0 = 9 \pm 1$ ; c) for **1a** only,  $A_1 = 26655 \pm 50$ ,  $t_1 = 10.46 \pm 0.03 \text{ (ns)}$ ,  $A_2 = 5690 \pm 8$ ,  $t_2 = 742 \pm 2 \text{ (ns)}$ ,  $y_0 = 12 \pm 1$ . Fast component is the instrumental response of TCSPC in THF. Long-time component is the excited state lifetime of **1a** in the corresponding solution.

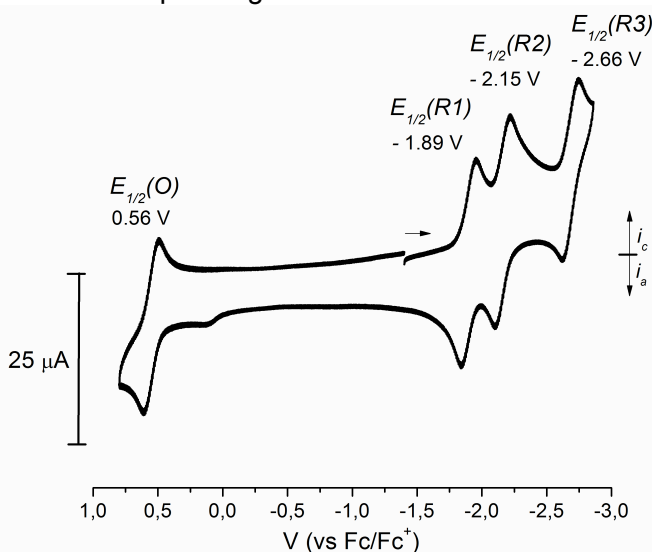


**Figure S18.** Cyclic voltammogram of **1b** at 100 mV/sec scan rate. The oxidation potential (O) and the reduction potentials (R1, R2, R3) are given as a half-wave potential.

**Spectroscopic data of 3.**

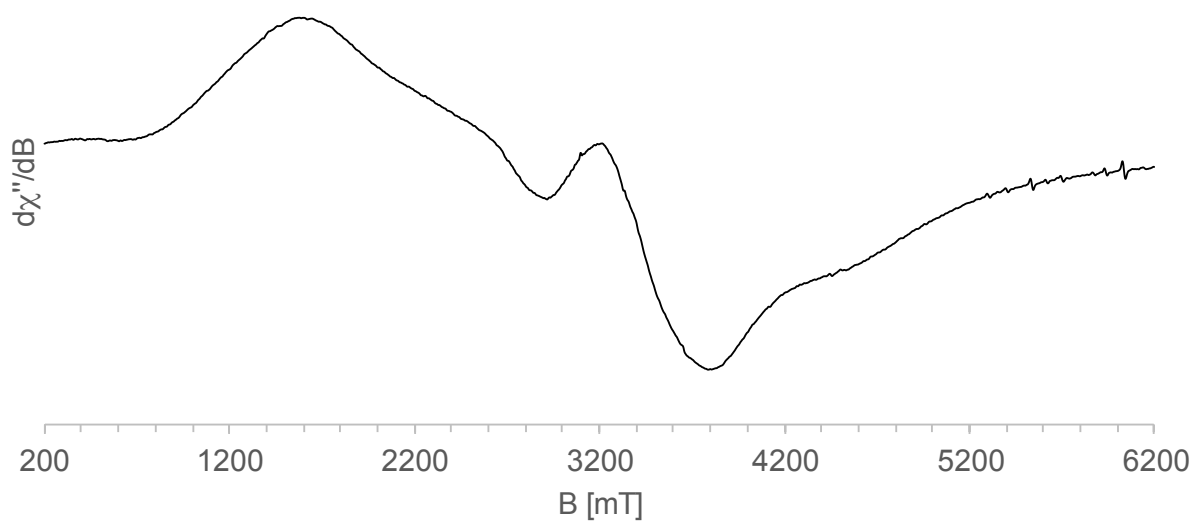


**Figure S19.** X-Band EPR spectrum of **3** recorded at 298 K in  $C_6D_6$  solution (microwave frequency = 9.377 GHz, power = 200 mW, power attenuation = 0.0 dB, modulation amplitude = 16.004 G).

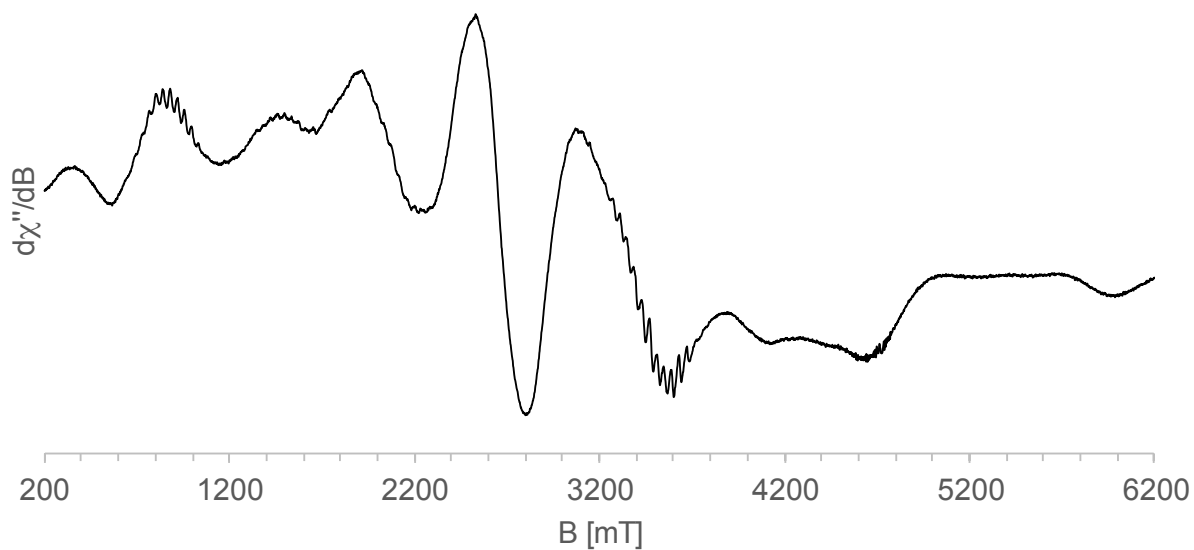


**Figure S20.** X-Band EPR spectrum of **3** recorded at 20 K in toluene glass (microwave frequency = 9.380 GHz, power = 2.00 mW, power attenuation = 20.0 dB, modulation amplitude = 4.000 G).

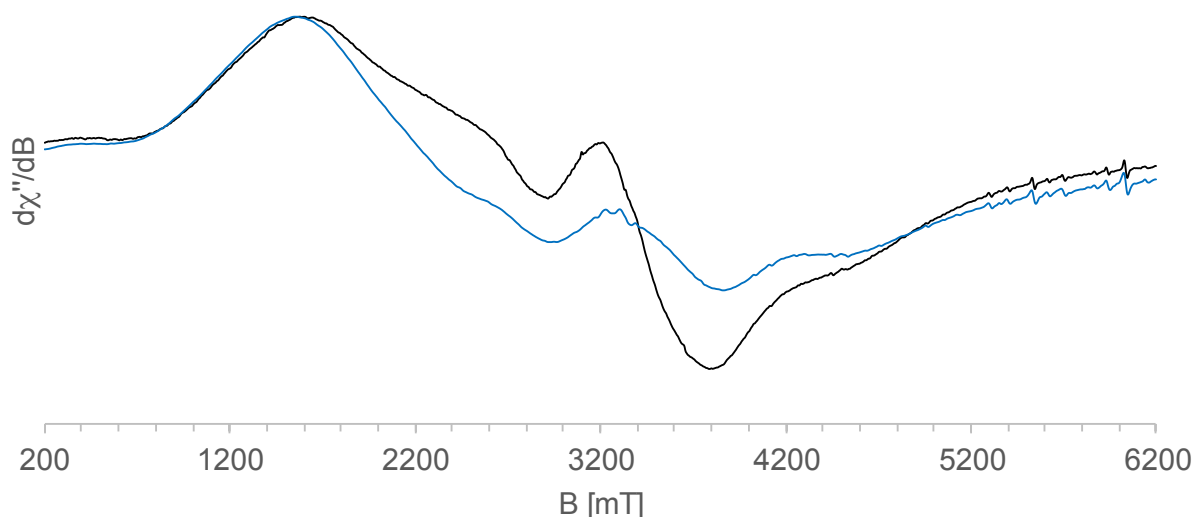


**Figure S21.** Black: X-Band EPR spectrum of **3** recorded at 298 K in  $C_6D_6$  solution (microwave frequency = 9.377 GHz, power = 200 mW, power attenuation = 0.0 dB, modulation amplitude = 16.004 G). Blue: X-Band EPR spectrum of the non-volatile residue of the catalytic reaction recorded at 298 K in  $C_6D_6$  solution (microwave frequency = 9.378 GHz, power = 200 mW, power attenuation = 0.0 dB, modulation amplitude = 16.004 G).

## References

- [1] A. B. Pangborn, M. A. Giardello, R. H. Grubbs, R. K. Rosen, F. J. Timmers, *Organometallics* **1996**, *15*, 1518-1520.
- [2] T. B. Hadda, H. Le Bozec, *Polyhedron* **1988**, *7*, 575-577.
- [3] M. P. Feth, C. Bolm, J. P. Hildebrand, M. Köhler, O. Beckmann, M. Bauer, R. Ramamonjisoa, H. Bertagnolli, *Chem. Eur. J.* **2003**, *9*, 1348-1359.
- [4] M. M. El'chaninov, A. A. Aleksandrov, V. A. Klushin, *Russian Journal of General Chemistry* **2016**, *86*, 1581-1583.
- [5] N. A. Yakelis, R. G. Bergman, *Organometallics* **2005**, *24*, 3579-3581.
- [6] G. R. Fulmer, A. J. M. Miller, N. H. Sherden, H. E. Gottlieb, A. Nudelman, B. M. Stoltz, J. E. Bercaw, K. I. Goldberg, *Organometallics* **2010**, *29*, 2176-2179.
- [7] B. J. Shields, B. Kudisch, G. D. Scholes, A. G. Doyle, *J. Am. Chem. Soc.* **2018**, *140*, 3035-3039.
- [8] A. Pannwitz, A. Prescimone, O. S. Wenger, *Eur. J. Inorg. Chem.* **2017**, *2017*, 609-615.
- [9] a) A. L. Chaney, E. P. Marbach, *Clinical Chemistry* **1962**, *8*, 130-132; b) W. T. Bolleter, C. J. Bushman, P. W. Tidwell, *Analytical Chemistry* **1961**, *33*, 592-594.
- [10] a) J.-P. Cheng, Y. Lu, X.-Q. Zhu, Y. Sun, F. Bi and J. He, *J. Org. Chem.*, 2000, **65**, 3853-3857; b) N. N. Voinovskaya, M. I. Terekhova, T. V. Sakhno, G. A. Val'kova, L. F. Rybakova, É. S. Petrov and A. I. Shatenshtein, *Chem. Heterocycl. Compd.*, 1982, **18**, 957-960.
- [11] F. G. Bordwell, J. Cheng, G. Z. Ji, A. V. Satish and X. Zhang, *J. Am. Chem. Soc.*, 1991, **113**, 9790-9795.